Journal of Power Sources 246 (2014) 473–481

Contents lists available at ScienceDirect

Journal of Power Sources

journal homepage: www.elsevier.com/locate/jpowsour

Partial oxidation of methane in an adiabatic-type catalytic reactor

A. Al-Musa [a,*], S. Shabunya [b], V. Martynenko [b], S. Al-Mayman [a], V. Kalinin [b], M. Al-Juhani [a], K. Al-Enazy [a]

[a] Energy Research Institute, King Abdulaziz City for Science and Technology (KACST), P.O. Box 6086, Riyadh 11442, Saudi Arabia
[b] State Scientific Institution "A.V. Luikov Heat and Mass Transfer Institute", National Academy of Sciences of Belarus, 15 P. Brovki, Minsk 220072, Belarus

HIGHLIGHTS

- Catalytic partial oxidation of methane was studied in adiabatic reactor.
- We examine four catalysts in POX processes of various methane/air mixtures.
- Similar characteristic residence time ~0.05 s is revealed for all catalysts.
- Composition of measured POX products was compared with developed model predictions.
- Measurements and modeling agree at temperature close to measured at catalyst outlet.

GRAPHICAL ABSTRACT

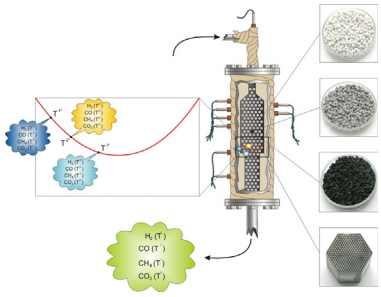

ARTICLE INFO

Article history:
Received 24 June 2013
Received in revised form
25 July 2013
Accepted 30 July 2013
Available online 9 August 2013

Keywords:
Partial oxidation
Steam reforming
Syngas
Adiabatic
Isothermal equilibrium

ABSTRACT

In the experimental setup designed for catalysts testing and development of technological modes, experiments on partial oxidation were carried out using four types of catalysts in the range of equivalence ratios from 2.2 to 6. The characteristic residence time of working mixture in the catalyst unit is ~0.05 s. The processing of experimental data indicates that the yield compositions may be explained by the radial temperature profile in the catalyst. For all the tested catalysts the measured yield composition is well approximated by averaging the isothermal equilibrium compositions calculated using the suggested temperature profile.

1. Introduction

The steadily growing interest in development of hydrogen energetics demands studies of hydrogen production. The demands of hydrogen energetics have risen interest in the most efficient conversion of hydrocarbons into a synthesis-gas (syngas). Among the variety of ways by which hydrogen production has been proposed [1,2], hydrogen generation in partial oxidation (POX) processes has garnered particular attention due to its exothermicity [2] and the possibility of implementing more compact productive installation design [3]. Application of thermal partial oxidation (TPOX) processes for hydrogen production in a non-catalytic porous media-based reformer [aluminum oxide (Al_2O_3) fiber static mixer structures and ceramic (SiC) foams] has been studied numerically and experimentally for methane [4]. TPOX results in a low hydrogen (H_2) yield (20%), and the preheating of air has no significant influence on syngas composition. Thermodynamics and kinetics of ethanol conversion have been theoretically investigated [5]. Thermal and chemical processes in a porous media-based reformer [4]

* Corresponding author. Tel.: +966 1 481 4316; fax: +966 1 481 3880.
E-mail address: aalmusa@kacst.edu.sa (A. Al-Musa).

0378-7753/$ – see front matter © 2013 Elsevier B.V. All rights reserved.
http://dx.doi.org/10.1016/j.jpowsour.2013.07.117

have been numerically simulated [6]. Modeling results of methane TPOX showed better agreement for Al_2O_3 rather than for SiC foam.

Yields of POX processes can be significantly enhanced using catalysts. Progress in manufacturing efficient new catalysts and improvement in the performance of commercially available catalysts stimulate investigations of hydrogen production in POX processes. By now the effect of different catalysts on the efficiency of hydrocarbon conversion in POX processes has only been partially studied. Catalytic partial oxidation (CPOX) of octane at 1100 °C for syngas production has been reported [7], and hydrogen generation from carbon (C_1–C_{10}) hydrocarbons at temperatures of 500–600 °C has been investigated [8]. In both studies, rhodium catalyst was used (7 wt% Rh [7] and 1 wt% Rh [8]). Further, CPOX of methane has been studied experimentally and numerically on Rh-coated foam [9]. Complete oxygen (O_2) conversion within 2 mm of the catalyst was found experimentally, while H_2 and carbon monoxide (CO) were formed both in the oxidation zone and by steam reforming after complete conversion of O_2.

Nickel (Ni)-based catalysts have been tested for POX of methane into a syngas [10,11]. The catalytic activity of $Ce_{1-x}Ni_xO_2$ catalysts has been investigated in oxidative steam reforming of propane [12]. Comparative studies of catalyst efficiency in POX of *n*-heptane have been conducted [13] to test Ni-based, rodium (Rh) and platinum (Pt) catalysts to assert that modified Ni-based/γ-Al_2O_3 catalyst exhibits both good catalytic activity and carbon deposition resistance ability. A proprietary noble metal catalyst has been used to extend the study of catalytic conversion on different hydrocarbon fuels (iso-octane, hexene, toluene, and gasoline) at steam-reforming and autothermal-reforming conditions [14]. The performance of chromium oxide catalysts supported on Al_2O_3 has been studied in the oxidative dehydrogenation of isobutane into isobutene at varying calcination conditions, pretreatment methods, and percents of chromium (Cr) loading [15]. Also oxidative dehydrogenation of isobutane has been studied with chromium-based mixed-oxide catalysts supported by alumina carriers [16]. The catalytic cracking of heavier hydrocarbons has also been studied [17].

Complete oxidation of methane (CH_4) over noble metal-based catalysts at low temperatures focusing on the abatement of CH_4 emissions has been reviewed in detail [18]. A review of catalysts used for catalytic combustion [19] has been expanded to methane and lower alkanes and has covered both low-temperature and high-temperature catalytic combustion. Though CPOX of methane to synthesis gas was studied in case of NiO catalysts [20] and Ni/CeO_2–ZrO_2 [21] in small-scale experimental installations, the study of methane CPOX processes with regimen parameters closer to those associated with industrial application is required.

The chemical process on catalysts with high selectivity implies a short contact time (sufficient to realize the principal reaction) with a subsequent rapid "quenching" of the non-equilibrium reaction products at the outlet of the catalyst. At the laboratory conditions, such requirements are fully realizable. Proceeding to the full-scale production, it is difficult to maintain the desired isothermal regimen within the entire volume of the catalyst. There are always temperature and concentration gradients with their values depending on density of heat fluxes (supporting "isothermal" regimen) and design solutions of the temperature control system. Some difficulties occur in case "quenching" of reaction products require rapid cooling, because the optimal contact time of gases with catalyst material is short and the process is very sensitive to changes in the catalytic properties (aging and degradation) and the process regimen. The traditional solution is a catalytic process that focuses on the equilibrium parameters of the mixture, which is easier to organize and operate. If there is an equilibrium with a suitable composition of the components and this equilibrium is reached under realizable conditions (temperature and pressure), the process can be managed using fairly simple catalysts. Partial oxidation of hydrocarbons in many applications can be carried out precisely using such an approach when the residence time of the gas mixture in a catalytic reactor is sufficiently high and the composition of yields is close to equilibrium.

In the King Abdulaziz City for Science and Technology, KACST, an experimental installation has been designed for systematic studies of POX catalytic processes. A general schematic diagram of the experimental installation to study these processes is shown in Fig. 1. Studies on this installation aim to test various catalysts and to develop effective technological modes for conversion of various hydrocarbons at conditions close to adiabaticity.

2. Materials and methods

The experimental bench consists of a gas-mixture preparation unit, a reactor, and a measuring system, controlled by a personal computer. A working mixture can be prepared using three gases: methane, air, and oxygen. Their flow rates are controlled by mass flow controllers (Omega 5400). Inlet gases are mixed in a receiver and supplied to a heater-evaporator, where flow of a liquid (water) can also be supplied. The value of the flow rate is controlled by a Bronkhorst mass flow controller. The liquid is evaporated in a heater/evaporator and mixed with gases. Controlled heating of the working mixture also occurs in this unit. After heating, the prepared mixture is supplied to a cylindrical reactor. The reactor vessel, which is made of steel (a stand is designed for the experiments at elevated pressure), has 124-mm inner diameter and 500-mm height. The inner thermal insulation is made of extruded kaolin wool, and the outer thermal insulation is made of kaowool blanket. The inner channel of the reactor consists of two parts: the upper (inlet gas) part (68 mm diameter and 180 mm length) and the lower part (46 mm diameter

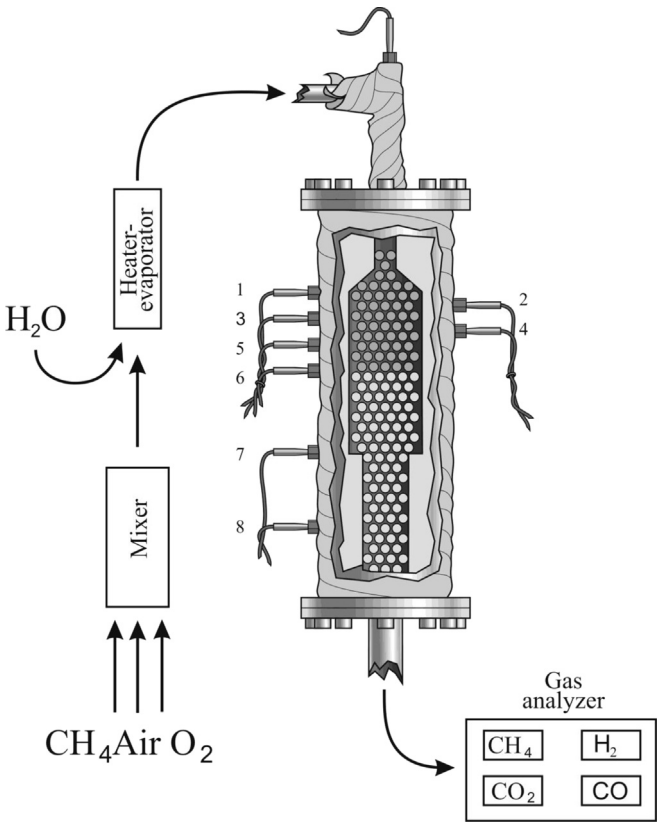

Fig. 1. General schematic of experimental system.

Table 1
Specifications of the catalysts.

	Carrier	Catalyst	%	[a]BET area $m^2\ g^{-1}$	Size, mm
a	γ-Al_2O_3	Rh	0.1	5.5	∅ 5
b	γ-Al_2O_3	Pt	0.5	82.3	∅ 3.2, $l = 3.6$
c	γ-Al_2O_3	Ni	Ni-synetix	91.5	$l = 3.5$, $h = 1$
d	α-Al_2O_3	ZrCe/LaNiPt			$\Delta = 1.5$

[a] BET area – Brunauer–Emmett–Teller surface area.

and 210 mm length). Part of the inner channel is filled with the catalyst being tested, and the remaining part contains inert filling Al_2O_3 grains characterized by mean size of 3.5 mm. A Labfacility K-type thermocouple is installed in this channel just below the flange to measure the temperature of the inlet mixture. Eight Labfacility K-type thermocouples are used to measure the temperature inside the working channel of the reactor. The first five thermocouples are equidistantly arranged 15 mm apart. The next is on a 30-mm stand, and the last two are on 90-mm stands. The numbering of the thermocouples is shown in Fig. 1.

The gas mixture leaving the reactor is cooled, dried, and supplied to the measuring system, which currently consists of three Edinburgh Instruments optical sensors determining the concentration of CO, CO_2 and CH_4, and a measurement technology katharometer to measure the concentration of H_2. In the experiments with methane, CH_4 concentration in the inlet mixture is also measured by an optical sensor. The main advantages of such a set of sensors are that they allow fast measurement, ease process control automations, and data acquisition.

In this study, we performed catalytic POX of methane–air mixtures with varying equivalence ratios (from 2 to 6) conducted at atmospheric pressure at the reactor outlet. In these experiments four catalysts were used. This set of results is used to describe the technique of measured data processing and presentation. The results of experiments with oxygen enrichment of air and addition of water will be discussed in forthcoming paper. In all experiments presented here, the heater was used for the reactor startup only. Initially, the catalyst bed was preheated up to 370 °C by hot air flow, a working mixture was supplied to the reactor, and the heater was switched off. Once the temperature of the working mixture at the reactor inlet decreased to room temperature (26 °C), the composition of the inlet mixture changed. At each fixed value of the equivalence ratio, stable readings of the sensors were recorded, and followed by the next working regimen of interest was made.

Three granular catalysts (Pt, Ni, and Rh) and one honeycomb type were tested in the experiments. The characteristics of catalysts used are given in Table 1 and the photos of the catalysts are shown in Fig. 2. All granular catalysts were supported on γ-Al_2O_3. The granular catalytic filling is between the level of the first thermocouple and the seventh (the volume of the catalytic filling is equal to 327 cm^3). The honeycomb unit was produced in Boreskov Institute of Catalysis SB RAS in the form of a regular polyhedron with diameter of 54 mm and height of 47 mm. It occupied the space between 1 and 4 thermocouples. Empty space around honeycomb catalyst was filled with kaowool.

3. Theory/calculations

Steady operation of the reactor at different ratios of the methane/air mixture was selected in the files containing the experimental data recordings. The value of the equivalence ratio $\gamma = 2C_{CH_4}/C_{O_2}$ was calculated for each of these intervals to characterize the excess of methane in the inlet mixture. Four volumetric concentrations measured in the dried outlet mixture were presented as a function of γ: $C_{H_2}(\gamma)$, $C_{CO}(\gamma)$, $C_{CO_2}(\gamma)$ and $C_{CH_4}(\gamma)$. Three temperatures were selected from the set of temperature

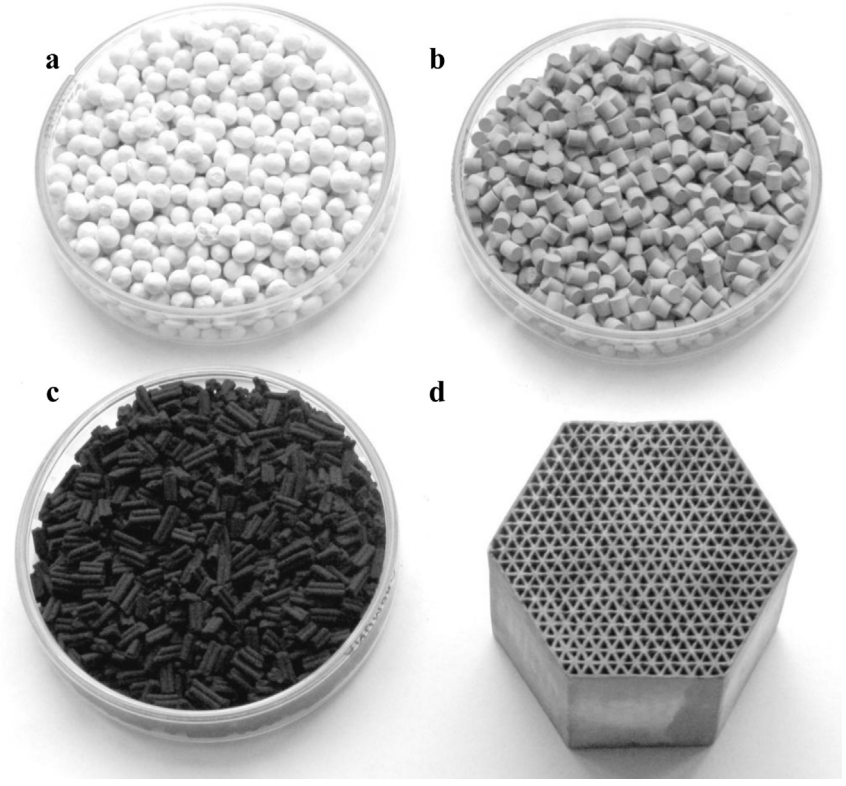

Fig. 2. Tested catalysts.

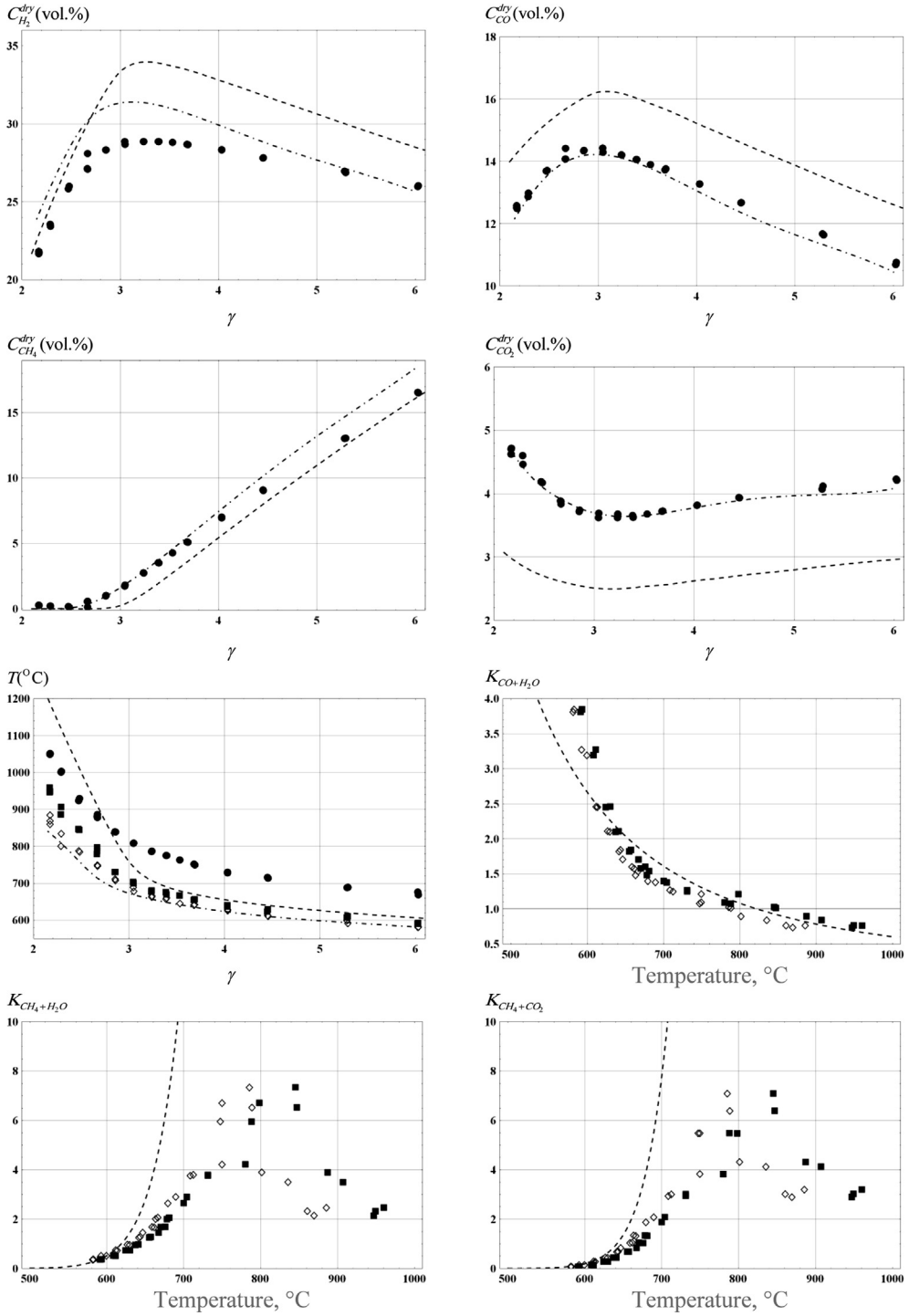

Fig. 3. Processing experiments with Ni as catalyst.

measurements: $T^{cat}_{in}(\gamma)$ – at catalyst inlet, $T^{cat}_{out}(\gamma)$ and $T^{inert}_{out}(\gamma)$ – at the outlet of catalytic and inert fillings, respectively. Different temperature maxima (hot spots) located in the inlet layer of the catalytic filling occurred at the same mixture composition as different catalysts were used. The value of this maximum depends on the balance of the exothermic and endothermic processes in the catalyst, and in some ways this balance is characterized by temperature $T^{cat}_{in}(\gamma)$.

The obtained experimental results were further processed in order to restore a "wet" concentration for comparison of mixture composition with the one at equilibrium conditions by three reactions:

$$CO + H_2O \leftrightarrow CO_2 + H_2, \quad (1)$$

$$CH_4 + H_2O \leftrightarrow CO + 3H_2, \quad (2)$$

$$CH_4 + CO_2 \leftrightarrow 2CO + 2H_2. \quad (3)$$

The procedure of functional minimization was used. It is based on the following hypotheses and conditions:

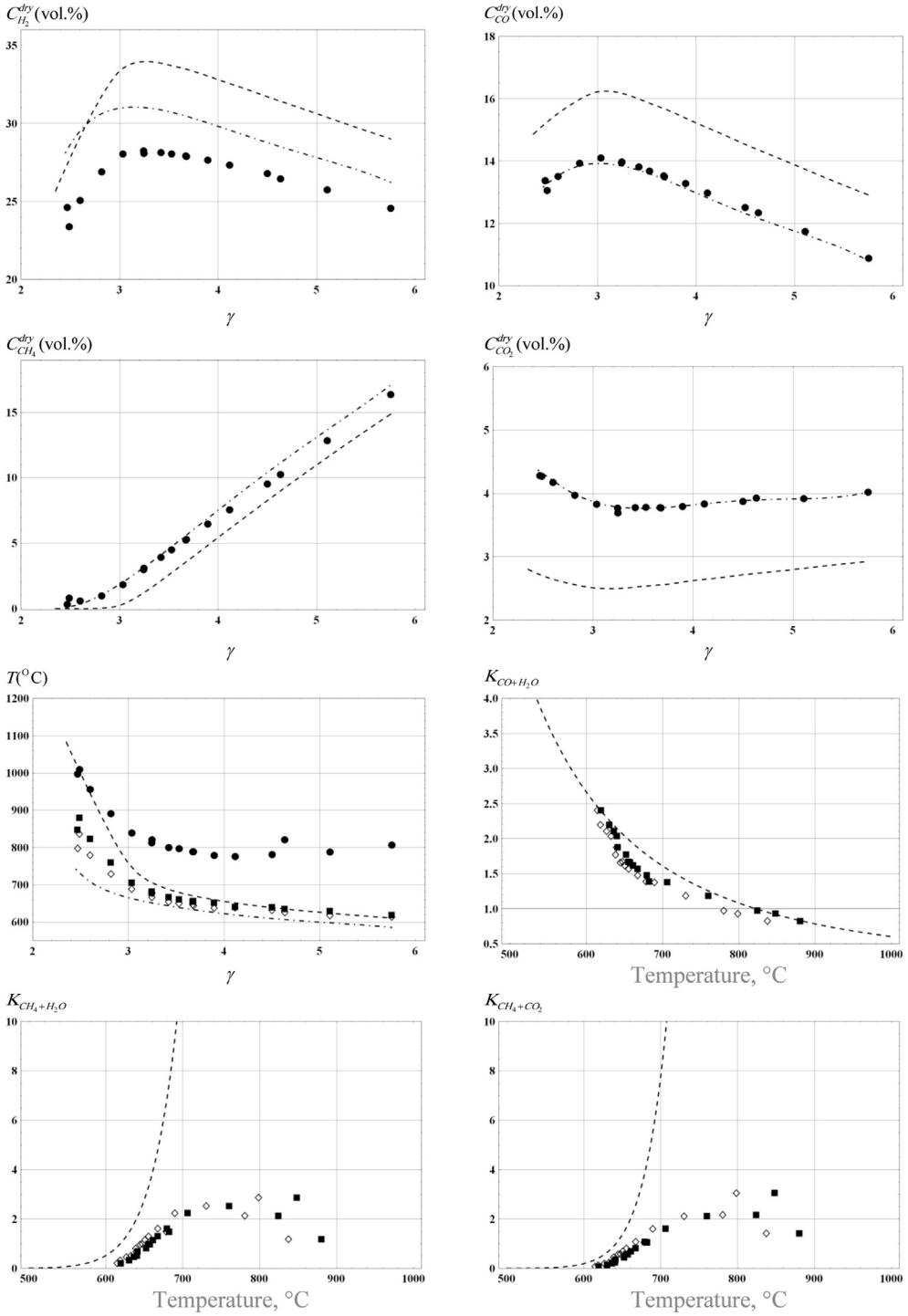

Fig. 4. Processing experiments with Pt as catalyst.

- The outlet mixture contains 7 components – H_2, CO, CO_2, CH_4, N_2, Ar, and H_2O.
- The outlet concentration of these components has to fulfill the N_2, Ar, C, O, and H balance inlet and outlet mixtures, and give the best matching of calculated and measured concentrations.

Using minimization procedure, the values of the stoichiometric coefficients n_{H_2}, n_{CO}, n_{CO_2}, n_{CH_4}, and n_{H_2O} were determined for the following reaction:

$$\mathrm{CH_4} + \frac{2}{\gamma}\mathrm{O_2} + \frac{2}{\gamma}\cdot\frac{78.08}{20.95}\mathrm{N_2} + \frac{2}{\gamma}\cdot\frac{100-99.03}{20.95}\mathrm{Ar} = n_{\mathrm{H_2}}\mathrm{H_2} + n_{\mathrm{CO}}\mathrm{CO} + n_{\mathrm{CO_2}}\mathrm{CO_2} + n_{\mathrm{CH_4}}\mathrm{CH_4} + \frac{2}{\gamma}\cdot\frac{78.08}{20.95}\mathrm{N_2} + \frac{2}{\gamma}\cdot\frac{100-99.03}{20.95}\mathrm{Ar} + n_{\mathrm{H_2O}}\mathrm{H_2O} \quad (4)$$

Further "balanced" dry $C_{H_2}^{dry}(\gamma)$, $C_{CO}^{dry}(\gamma)$, $C_{CO_2}^{dry}(\gamma)$, and $C_{CH_4}^{dry}(\gamma)$, and wet $C_{H_2}^{wet}(\gamma)$, $C_{CO}^{wet}(\gamma)$, $C_{CO_2}^{wet}(\gamma)$, $C_{CH_4}^{wet}(\gamma)$, and $C_{H_2O}^{wet}(\gamma)$ volumetric

concentrations were computed. Values of the reaction equilibrium constants calculated for the reactions (1)–(3) were compared to the concentration ratios of outlet mixture components:

$$K_{CO+H_2O} = \frac{C_{CO_2}^{wet} C_{H_2}^{wet}}{C_{CO}^{wet} C_{H_2O}^{wet}},\quad K_{CH_4+H_2O} = \frac{C_{CO}^{wet}\left(C_{H_2}^{wet}\right)^3}{C_{CH_4}^{wet} C_{H_2O}^{wet}},$$
$$K_{CH_4+CO_2}(\gamma) = \frac{\left(C_{CO}^{wet}\right)^2\left(C_{H_2}^{wet}\right)^2}{C_{CH_4}^{wet} C_{CO_2}^{wet}}. \quad (5)$$

The calculations were conducted for temperature $T_{out}^{cat}(\gamma)$ (■) and $T_{out}^{inert}(\gamma)$ (◇). For comparison, the characteristics of adiabatic and the "nearest" isothermal equilibrium were calculated. They are temperatures $T_{ad}(\gamma, T_0)$ and $T_{lz}(\gamma, T_0)$ and concentrations $C_{i\_ad}(\gamma, T_0)$ and $C_{i\_lz}(\gamma, T_{lz}(\gamma, T_0))$ corresponding to the adiabatic equilibrium and to their "nearest" isothermal equilibrium, respectively. Temperature $T_{lz}(\gamma, T_0)$ is selected to approach equilibrium composition as close as possible to the experimentally measured values $C_{H_2}(\gamma)$,$C_{CO}(\gamma)$, $C_{CO_2}(\gamma)$, and $C_{CH_4}(\gamma)$.

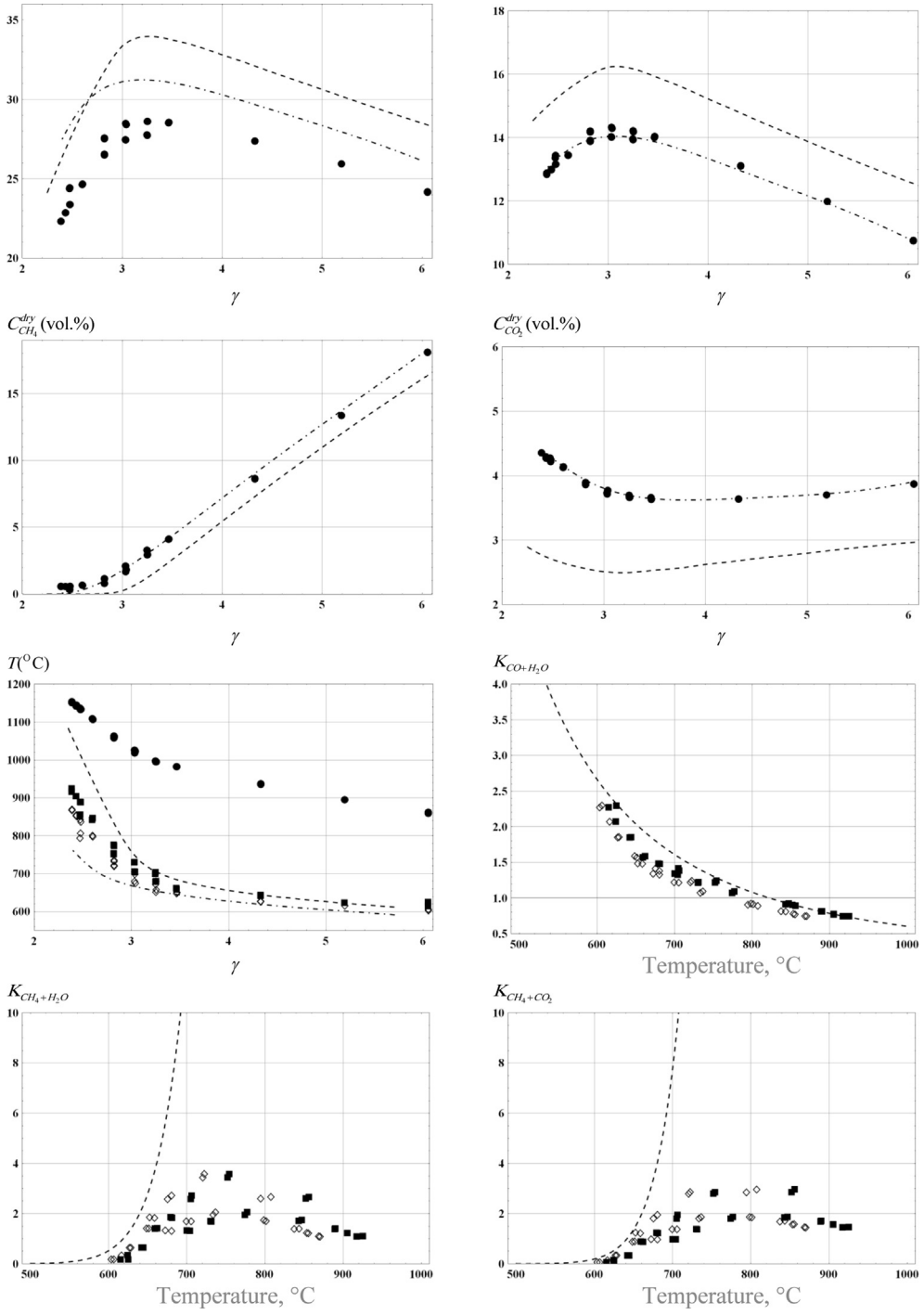

Fig. 5. Processing experiments with Rh as catalyst.

4. Results

The results of this processing were performed as a set of eight graphs for each catalyst tested (Figs. 3–6). Four graphs of concentration data and one of temperature are the function of γ, while three graphs of equilibrium constants versus temperature were plotted. Experimental measurements are shown by symbols while dashed and dot-dashed curves are the calculation of adiabatic and "nearest" isothermal equilibriums, respectively. In the graphs of temperature data symbols (●) correspond to temperature measurements in the inlet layer of the catalyst bed; symbols (■) and (◇) are the measurements at the outlet of the catalyst bed and the inert filling accordingly. In the last three graphs of each set, the comparison of the thermodynamic calculation of reaction equilibrium constants for reactions (1)–(3) with ratio of concentrations (5) is given.

In all experiments, the measured concentrations differed significantly from the calculation of adiabatic equilibrium, and were in a good agreement with the model of the "nearest" isothermal equilibrium, especially for CO, CO_2, and CH_4

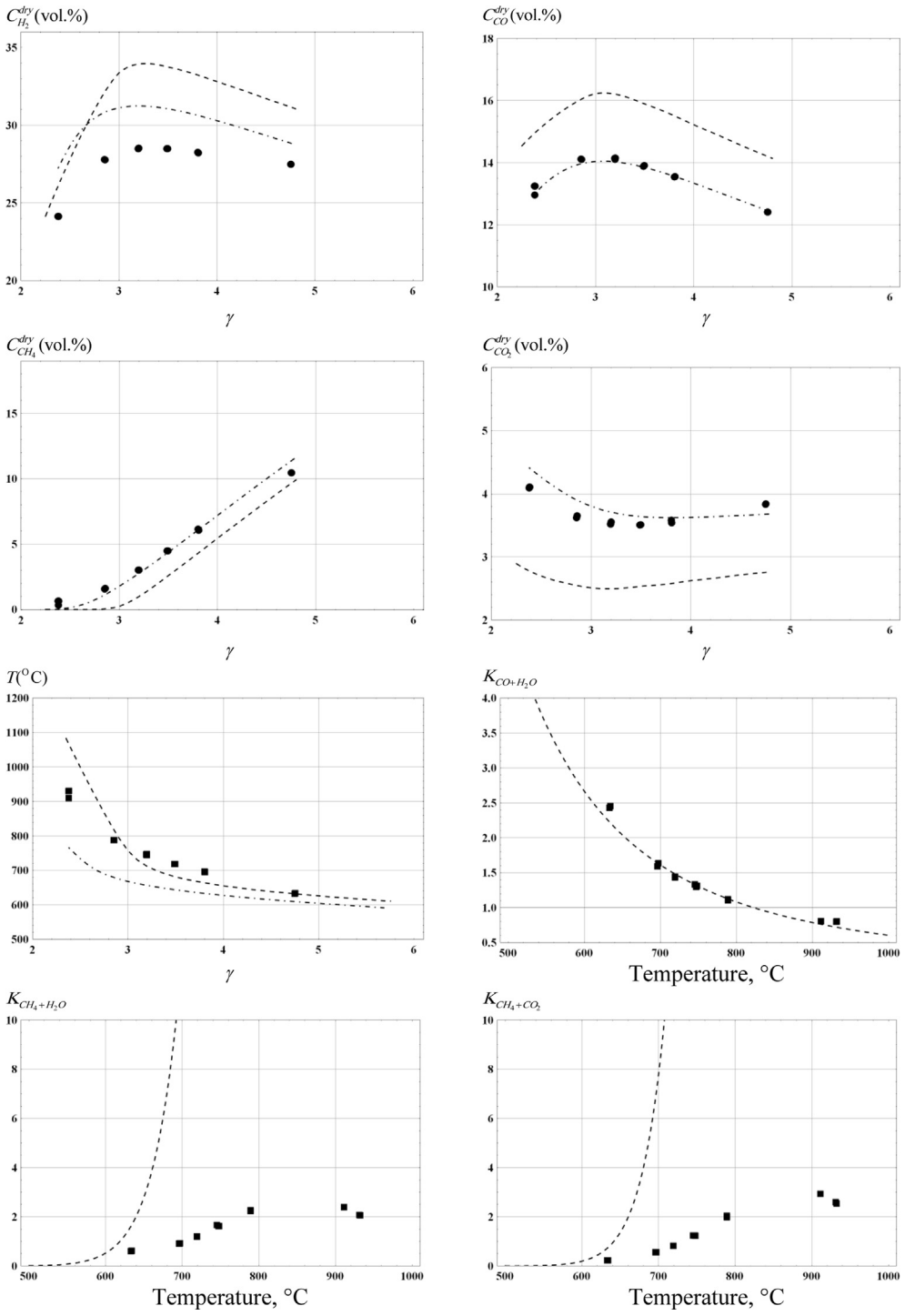

Fig. 6. Processing experiments with honeycomb as a catalyst.

components. A higher deviation in case of hydrogen could be explained partially by the inaccurate method of measuring H_2 concentration in a multicomponent mixture by katharometer. On the other hand, the essential deviation is observed for the component having the highest concentration.

The calculated temperatures $T_{Iz}(\gamma, T_0)$ were below the adiabatic equilibrium. This difference might be attributed to thermal losses. However, these temperatures were lower than $T_{out}^{cat}(\gamma)$, and in some places even lower than $T_{out}^{inert}(\gamma)$. In case of the "cold" regimen with high γ all three temperatures were almost equal; however, variations became apparent in hotter regimens with a lower γ. Homogeneous kinetics at temperatures $T_{out}^{cat}(\gamma)$ was slow, and one can assume that the chemical processes stopped when mixture left the catalyst. An estimation of the proximity of reaction (1) to the equilibrium shows that within the experimental accuracy an equilibrium is equally satisfied when both temperature $T_{out}^{cat}(\gamma)$ and $T_{out}^{inert}(\gamma)$ are used. In case of reactions (2) and (3), the use of a lower temperature $T_{out}^{inert}(\gamma)$ shifts the points closer to the equilibrium curve. However, even at $T_{Iz}(\gamma, T_0)$ calculated points do not fall within the equilibrium curve. Imbalance in these endothermic reactions was expected; however, the degree of deviation should be adjusted in terms of measurement errors of the hydrogen concentration and errors of the procedure recovering wet concentrations.

Since the composition of the outlet mixture was close enough to the isothermal equilibrium composition at temperature $T_{Iz}(\gamma, T_0) < T_{out}^{cat}(\gamma)$, it is possible to explain this result by a nonuniform radial temperature profile in the catalytic unit. The heads of thermocouples measuring temperatures $T_{out}^{cat}(\gamma)$ and $T_{out}^{inert}(\gamma)$ were along the reactor axis; therefore, they indicated the maximum temperature of the cross section. The decrease in temperature occurred due to thermal losses with distance from the axis. A simple parabolic approach for the temperature profile $T_{out}^{cat}(\gamma, r, a) = T_{out}^{cat}(\gamma) - ar^2$ can be used at the catalyst bed outlet. This profile satisfies the symmetry condition at $r = 0$, and has one unknown parameter a, which characterizes thermal losses. For the sake of assessment, it can be assumed that the catalyst was quite active, so an isothermal equilibrium was present at $T_{out}^{cat}(\gamma, r, a)$ in each point of the cross section (*i.e.*, concentrations in this section $c_{i\_Iz}(\gamma, T_{out}^{cat}(\gamma, r, a))$ were also functions of the radius).

In this model, the mixture composition measured at the reactor outlet was the result of averaging over the cross section. The temperature profile caused a redistribution of mass flows in the cross section, and strictly speaking, it was necessary to solve the problem of a two-dimensional filtration to determine the radial distribution of the axial velocity. To make a simple estimation, it was assumed that the axial velocity component was independent of the radius and the mass redistribution was only due to a change in density $\rho_{i\_Iz}(\gamma, T_{out}^{cat}(\gamma, r, a))$. This was also obtained by calculation of the equilibrium. In this approximation, the average mass concentration of the components was written as the ratio of two integrals:

$$c_{i\_av} = \frac{\int_0^R c_{i\_Iz}(\gamma, T_{out}^{cat}(\gamma, r, a))\rho_{i\_Iz}(\gamma, T_{out}^{cat}(\gamma, r, a))r\mathrm{d}r}{\int_0^R \rho_{i\_Iz}(\gamma, T_{out}^{cat}(\gamma, r, a))r\mathrm{d}r} \quad (6)$$

where R is the radius of catalyst bed. When the average concentration of the four components was closest to the experimental values, the optimal value a_{opt} could be found by varying the parameter a. If these assumptions are correct, the average temperature

$$T_{out\_av}^{cat} = \frac{\int_0^R Cp_{i\_Iz}(\gamma, T_{out}^{cat}(\gamma, r, a_{opt}))T_{out}^{cat}(\gamma, r, a_{opt})\rho_{i\_Iz}(\gamma, T_{out}^{cat}(\gamma, r, a_{opt}))r\mathrm{d}r}{\int_0^R Cp_{i\_Iz}(\gamma, T_{out}^{cat}(\gamma, r, a_{opt}))\rho_{i\_Iz}(\gamma, T_{out}^{cat}(\gamma, r, a_{opt}))r\mathrm{d}r} \quad (7)$$

should be close to $T_{Iz}(\gamma, T_0)$.

Indeed calculations performed for a_{opt} and $T_{out\_av}^{cat}$ demonstrated that $T_{out\_av}^{cat}$ and $T_{Iz}(\gamma, T_0)$ were almost the same for the four tested catalyst samples in all regimens. Using the model with a parabolic temperature profile, the dependence of concentrations on γ remained almost unchanged, *i.e.*, $C_{i\_av} \approx C_{i\_Iz}(\gamma, T_{Iz}(\gamma, T_0))$. By implication, a parabolic profile should allow for a better approximation of the results, rather than average temperatures; however, within the error in the concentration measurements and dimensions of the used catalyst samples, these two approaches were equivalent. The temperature difference between the axis and the radius at the catalyst outlet $\delta T = a_{opt}R^2$ as a function of γ is shown in Fig. 7. Calculated dependence of the power of thermal losses from catalyst $W_{Therm\ losses}$ on γ is shown in Fig. 8.

$$W_{Therm\ losses} = G_{mix}\delta H(\gamma, T_0), \quad (8)$$

where $\delta H(\gamma, T_0) = H(\gamma, T_0) - H[C_{i\_Iz}(\gamma, T_{Iz}(\gamma, T_0)), T_{Iz}(\gamma, T_0)]$.

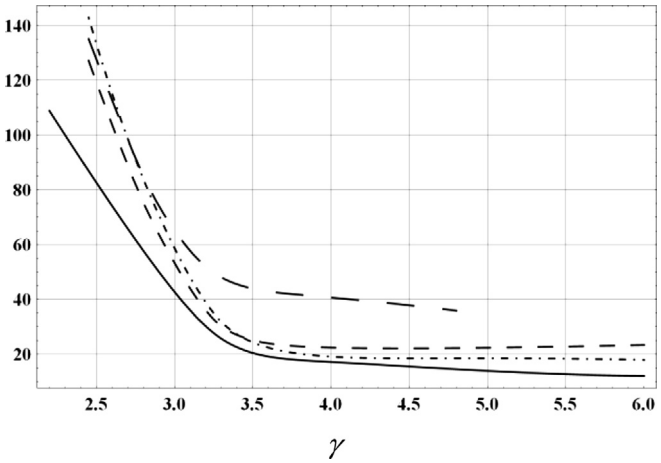

Fig. 7. Effect of varying γ on δT calculated for different catalysts: (—— – Ni, - - - - – Pt, -·-·- – Rh, – – – – honeycomb).

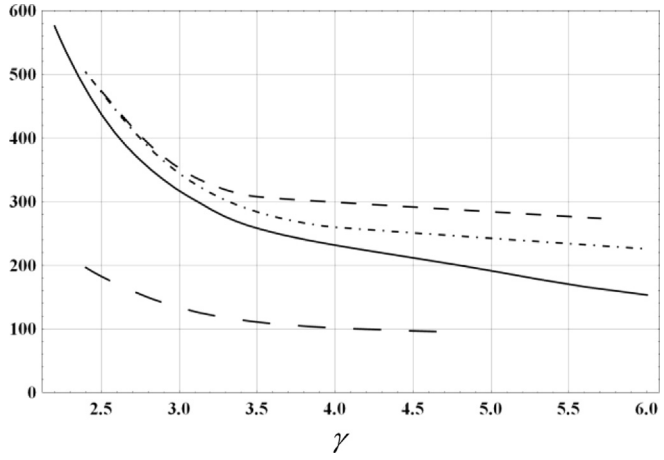

Fig. 8. Thermal losses calculated for different catalysts at varying γ: (—— – Ni, - - - - – Pt, -·-·- – Rh, – – – – honeycomb).

The dependence of thermal characteristics δT and $W_{\text{Therm losses}}$ on γ was similar and clear for all tested catalyst samples. The hotter the conditions, the bigger were the losses. In hot regimens at $\gamma < 3$ the values of δT mainly depended on the scale of the "hot spot" and minimum values of this parameter were attributed to the nickel catalyst. This result does not characterize the properties of actual metals, but it is attributed to catalysts (e.g., activity of metal, number of catalytic sites on the grain surface, and size and shape of the grain).

The noticeable difference in behavior of the honeycomb catalyst sample among the three catalysts was due to the honeycomb structure. Flow in each channel of the honeycomb catalyst is separated from each other and heat conductivity occurred through the walls only. In bulk catalysts the pattern of filtration is much more complex. The effective transverse thermal conductivity is higher and therefore, thermal losses are reduced in case of honeycomb catalyst. With regard to the temperature difference, it would be necessary to use a more flat temperature profile instead of a parabola for simulation of the processes in the honeycomb catalyst.

5. Conclusion

Four types of catalysts were tested in terms of hydrocarbons partial oxidation within the wide range of methane–air compositions ($2.2 \leq \gamma \leq 6$). The characteristic temperatures at the outlet of the catalytic unit were within the range of 600–950 °C. The typical residence time of the gas mixture inside the catalytic unit was 0.05 s. The experimental data processing for the four tested catalyst samples revealed that in all the studied regimes the composition of the outlet mixture was very close to the equilibrium composition at average temperatures of mixture at the catalyst bed outlet. The temperature profile in the catalytic unit was controlled by thermal losses. Therefore, the higher the temperature of the adiabatic equilibrium, the larger the deviation was from adiabaticity.

Since equilibrium composition is observed even at experimental conditions employing the lowest temperature approximately 580 °C, it means that the amount of catalyst used is at least "sufficient" for such temperature. In case of the hot regimens, such an amount of catalyst is probably "redundant". Excessive amounts of catalyst (for an adiabatic type reactor) refer to the case where a local thermodynamic equilibrium is realized in a substantial volume of the outlet part of the catalyst. Hence, this part of the volume lowers the effective temperature equilibrium due to the thermal losses that affect conversion quality. The decrease of catalyst volume down to the "optimal" level will save the catalyst, and also will have a positive impact on the product composition.

Catalytic reactors operating in a local equilibrium (related to the temperature field in the outlet catalyst layer) mode do not require kinetic calculations since product composition is completely determined by inlet mixture composition and temperature. In the design of these reactors, it is necessary to organize the filtration and heat exchange in the catalytic unit to realize the required temperature in the outlet part of the catalyst. There are two ways to implement a target temperature. In case of "isothermal" reactor, steady temperature of the process should be maintained by heating of the catalytic unit. Therefore, the inlet mixture is usually supplied at room temperature or slightly heated. Another option is setting conditions for the catalytic unit close to adiabatic conditions. This requires heating the working mixture so that the temperature of the adiabatic equilibrium is consistent with the target temperature. In the former case, the difficulties associated with inhomogeneous heating are aggravated by the behavior of the filtration redistributing flow into the cold region. The temperature gradient in such schemes is inevitable, because energy is transferred from the walls deeper inside the filling. In latter variant, the temperature profile is due to imperfect passive insulation. Increase of the reactor diameter or specific flow rate of the reactive mixture makes the situation worse in the first scheme, while in the second one it is improved. Data from experiments with different preheating of the inlet mixture, varying the mixture flow rate, and controlling the diameter of catalyst bed are being prepared for submission.

Acknowledgments

We are grateful for all the support for this research work provided by King Abdulaziz City for Science and Technology, Saudi Arabia.

References

[1] M. Steinberg, H. Cheng, Int. J. Hydrogen Energy 14 (11) (1989) 797–820.
[2] Z. Al-Hamamre, http://www.scitopics.com/Hydrogen_Production.html, 2011.
[3] T. Riis, E.F. Hagen, P.J.S. Vie, Ø. Ulleberg, HIA_HCG_Production_2005-03-15_rev1_final.doc.
[4] Z. Al-Hamamre, S. Voß, D. Trimis, Int. J. Hydrogen Energy 34 (2) (2009) 827–832.
[5] Z. Al-Hamamre, M.A. Hararah, Int. J. Hydrogen Energy 35 (11) (2010) 5367–5377.
[6] Z. Al-Hamamre, A. Al-Zoubi, D. Trimis, Combust. Theory Model. 14 (1) (2010) 91–103.
[7] A. Anumakonda, J. Yamanis, J. Ferrall, US Patent 6,221,280, 2001.
[8] E. Newson, T.B. Truong, Int. J. Hydrogen Energy 28 (12) (2003) 1379–1386.
[9] R. Horn, K.A. Williams, N.J. Degenstein, L.D. Shmidt, J. Catal. 242 (2006) 92–102.
[10] Y. Chen, W. Zhou, Z. Shao, N. Xu, Catal. Commun. 9 (6) (2008) 1418–1425.
[11] A.T. Ashcroft, A.K. Cheetham, J.S. Foord, et al., Nature 344 (1990) 319–321.
[12] L. Pino, A. Vita, F. Cipitì, M. Laganà, V. Recupero, Catal. Lett. 122 (2008) 121–130.
[13] R. Ran, G. Xiong, S. Sheng, W. Yang, et al., Catal. Lett. 88 (1–2) (2003) 55–59.
[14] S. Springmann, G. Friedrich, M. Himmenb, M. Sommerb, G. Eige, Appl. Catal. A: Gen. 235 (2002) 101–111.
[15] S.M. Al-Zahrani, N.O. Elbashir, A.E. Abasaeed, M. Abdulwahed, Ind. Eng. Chem. Res. 40 (2001) 781–784.
[16] N.O. Elbashir, S.M. Al-Zahrani, A.E. Abasaeed, M. Abdulwahed, Chem. Eng. Proc. 42 (2003) 817–823.
[17] K.A. Mahgoub, S. Al-Khattaf, Energy & Fuel 19 (2) (2005) 329–338.
[18] P. Gelin, M. Primet, Appl. Catal. B: Environ. 39 (2002) 1–37.
[19] T.V. Choundary, S. Banerjee, V.R. Choundhary, Appl. Catal. A: Gen. 234 (2002) 1–23.
[20] H.Y. Wang, E. Ruckenstein, J. Catal. 199 (2001) 309–317.
[21] T. Takeguchi, S. Furukawa, M. Inoue, J. Catal. 202 (2001) 14–24.